The Free Internet Journal for Organic Chemistry

Paper

Archive for Organic Chemistry

Arkivoc **2017**, part iii, 166-180

Electrochemical reduction, radical anions, and dehalogenation of fluorinated/chlorinated 2,1,3-benzothia/selenadiazoles

Leonid A. Shundrin,*[a,b] Irina G. Irtegova,[a] Pavel A. Avrorov,[a] Tatiana F. Mikhailovskaya,[a] Arkady G. Makarov,[a] Alexander Yu. Makarov,[a] and Andrey V. Zibarev*[a,c]

[a]*Institute of Organic Chemistry, Russian Academy of Sciences, 630090 Novosibirsk, Russia*
[b]*Department of Natural Sciences, National Research University – Novosibirsk State University, 630090 Novosibirsk, Russia*
[c]*Department of Chemistry, National Research University – Tomsk State University, 634050 Tomsk, Russia*
E-mail: zibarev@nioch.nsc.ru, shundrin@nioch.nsc.ru

Dedicated to Prof. Oleg A. Rakitin on the occasion of his 65th birthday

Received 03-27-2017 **Accepted** 05-01-2017 **Published on line** 06-25-2017

Abstract

At the first stage of electrochemical reduction in DMF, fluorinated/chlorinated 2,1,3-benzothia/selenadiazoles formed long-lived radical anions characterized by EPR and DFT. Gas-phase electron affinities (EA_1) from DFT correlated well with the first-peak potentials separately for S and Se derivatives, and the latter were found to be better electron acceptors than the former in contrast to the atomic EA_1 and Allen electronegativity. At the second stage, chalcogen- and halogen-dependent dehalogenation proceeded: *non-hydro*defluorination of selenadiazoles through their n-electron activation (n ≥ 2), and *hydro*dechlorination of thia/selenadiazoles through H^+ addition to their dianions. These differ from dehalogenation of related (aza) aromatics (*e.g.* benzenes, naphthalenes, quinoxalines).

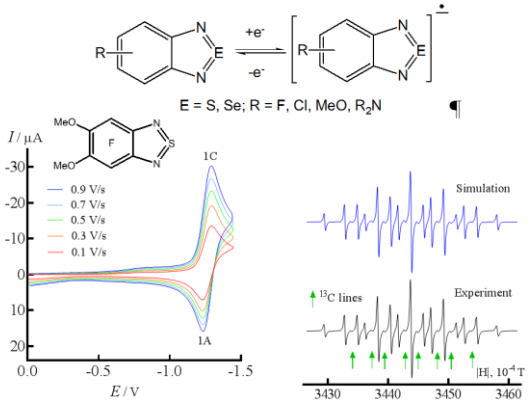

Keywords: 2,1,3-Benzothiadiazoles, 2,1,3-benzoselenadiazoles, chlorinated, cyclic voltammetry, dehalogenation, DFT, EPR, fluorinated, radical anions

 ©ARKAT USA, Inc

Introduction

2,1,3-Benzothia/selenadiazoles are redox-active 10π-electron heteroaromatics – chalcogen-nitrogen analogs of naphthalene and chalcogen analogs of quinoxaline.[1,2] Their chemistry is well-studied (for selected works, see refs. 3-10 and references therein). Similar to many other chalcogen-nitrogen π-heterocycles, they possess positive electron affinity (EA) making them effective electron acceptors[3] – precursors of stable radical anions (RAs) isolated in the form of salts and characterized by X-ray diffraction.[11,12] Also, they are luminophores. For these reasons, 2,1,3-benzothia/selenadiazoles found numerous applications as electron-acceptor or/and luminescent building blocks of real or potential molecular functional materials for electronics, optoelectronics and photovoltaics.[4,5,13-25] Despite fluorinated (hetero) aromatics are promising for electronic and optoelectronic applications,[26,27] fluorinated 2,1,3-benzothia/selenadiazoles are less studied in this context.

Hydrogen replacement by fluorine affects many properties of (hetero) aromatics including (hetero) aromaticity itself.[28] Particularly, it enlarges EA_1 of 2,1,3-benzothia/selenadiazoles,[2,3] *i.e.* their electron-acceptor ability, which can be used in the design of functional materials. Recently, our group suggested unified synthetic approach to fluorinated 2,1,3-benzothia/selenadiazoles.[29,30] Since redox properties of compounds are of general significance for organic chemistry and its applications,[31] in this work we report on electrochemical reduction (ECR) of new fluorinated 2,1,3-benzothia/selenadiazoles bearing also chlorine and some other substituents (**1**-**20**, Figure 1), studied by cyclic voltammetry (CV), as well as on their persistent RAs characterized by EPR spectroscopy and DFT calculations. Compounds **3** and **12** together with their RAs have been characterized earlier[2] as well as related fluorinated 1,4-benzodiazines (quinoxalines) and their RAs.[32] For some derivatives, chalcogen- and halogen-dependent dehalogenation was observed being of special chemical interest.

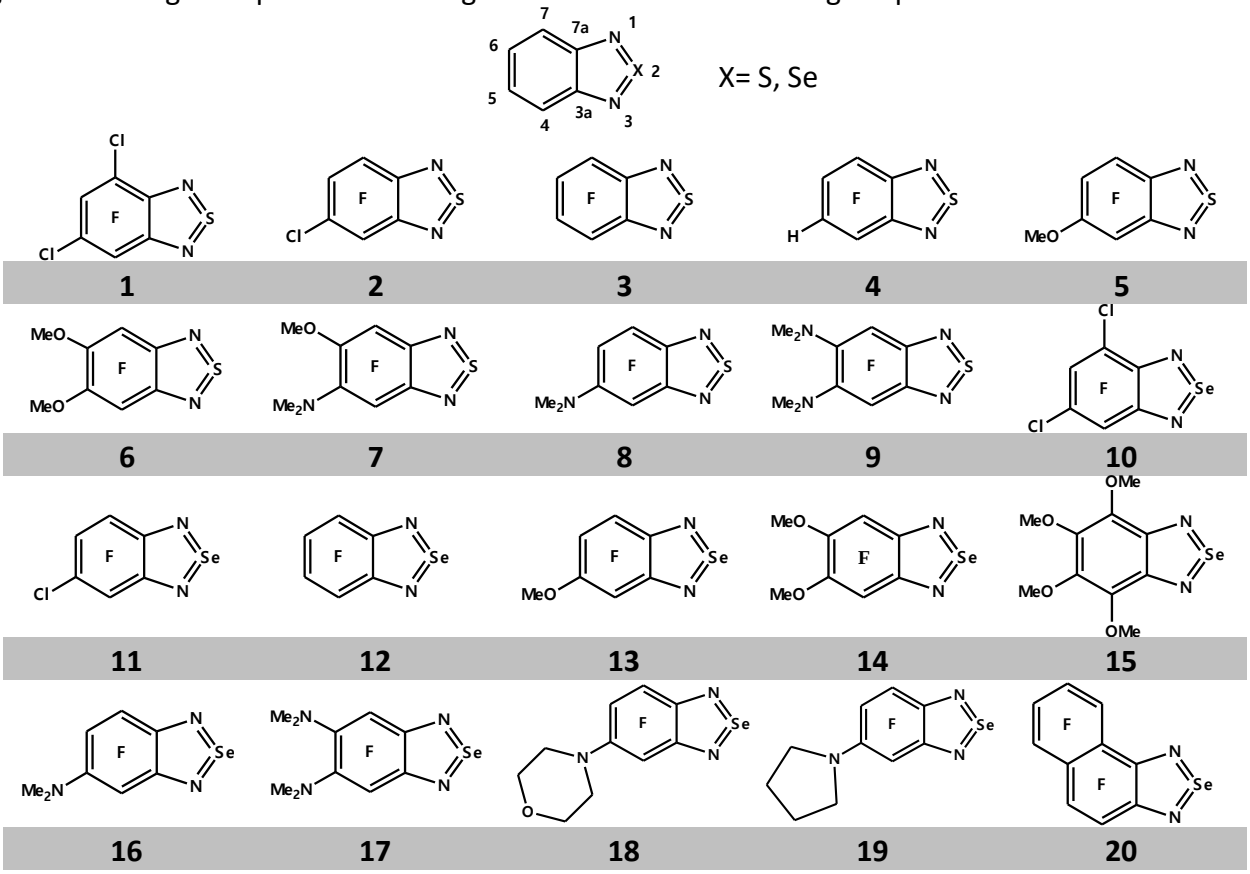

Figure 1. Compounds and atom numbering.

Results and Discussion

©ARKAT USA, Inc

Electrochemical reduction and dehalogenation. Most of the studied compounds are known ones.[29,30] Derivatives **1**, **2** and **4-9** were prepared by nucleophilic substitution of fluorine in 4,5,6,7-tetrafluoro-2,1,3-benzothiadizole **3**, and **10**, **11** and **13-19** in 4,5,6,7-tetrafluoro-2,1,3-benzoselenadiazole **12**. ECR peak potentials, CVs and some transformations of **1**-**20** under ECR in DMF in the potential range 0 > E > −2.2 V (vs. saturated calomel electrode, SCE) are represented in Table 1, Figures 2 and 3 (ESI: Figures S1 and S2, Table S1), and Schemes 1 and 2; for ECR of **3** in MeCN, see ref. 2. In E_p^{ij} designation of peak potentials, *i* is a number of peak and *j* = *C* or *A* indicates a cathode or an anode branches of CVs; designation of peak currents is the same.

Table 1. ECR peak potentials E_p^{iC} (V) in DMF[a] and gas-phase EA_1 (eV)[b] of compounds **1**-**20**

Compound		**1**	**2**	**3**	**4**	**5**	**6**	**7**
E_p^{iC}	*i* = 1	−1.00	−1.02	−1.11[c]	−1.12	−1.20	−1.30	−1.34
	i = 2	−1.94	−2.01		−2.27	~−2.4		
	i = 3	−2.19						
EA_1		1.67	1.63	1.57	1.57	1.36	1.16	1.07
Compound		**8**	**9**	**10**	**11**	**12**	**13**	**14**
E_p^{iC}	*i* = 1	−1.26	−1.39	−0.91	−0.94	−0.98	−1.08	−1.18
	i = 2			−1.71	−1.78	−1.97	−2.17	−2.20
	i = 3			−2.00[d]	−2.03	−2.05		
EA_1		1.28	1.01	1.81	1.78	1.72	1.55	1.30
Compound		**15**	**16**	**17**	**18**	**19**	**20**	
E_p^{iC}	*i* = 1	−1.38	−1.13	−1.28	−1.10[e]	−1.20	−1.08	
	i = 2	−2.30		−2.14	−2.06	−1.80	−1.09	
	i = 3					−2.07	−2.00	
EA_1		1.12	1.54	1.17	1.61	1.36	1.78	

[a] Measured with ν = 0.1 V.s^{-1}. [b] The first adiabatic EA calculated at the (U)B3LYP/6-31+G(d) level of theory.

[c] Recalculated from the data of ref. 2: E_p^{1C} (DMF) = E_p^{1C} (MeCN) + 0.1 (V). [d] An additional peak was observed at E_p^{4C} = −2.08 V (ESI, Figure S2). [e] ESI, Figure S2.

The first stage of the ECR of thiadiazoles **1-9** is one-electron transfer forming long-lived RAs characterized by EPR (see below). It features reversible and diffusion-controlled peaks in the CVs ($I_p^{1C} \cdot \nu^{-1/2}$ = const; ESI: Figures S1 and S2, Table S1). The ECR of **2** (Figure 2) is characterized by two peaks 1C and 2C at the first cycle of the CV, 0 > E > −2.2 V, the first of which is one-electron and reversible; no additional peaks were observed in the range 0 > E > −1.5 V covering the first step of the ECR only. The irreversible one-electron peak 2C corresponds to the formation of unstable dianion (DA) which can undergo an addition of two H^+ to N atoms (*cf.* ref. 33) or one H^+ to the carbocycle with subsequent hydrodechlorination. For **2**, the latter process seems to be slow because the reversible peaks 3C and 3A (E_p^{3C} = −1.12, E_p^{3A} = −1.07 V) corresponding to the formation of the RA of hydrodechlorinated product **4** (detected by EPR) were observed at the second and subsequent potential sweep cycles only with ν > 0.3 V·s^{-1} in the range 0 > E > −2.2 V (Figure 2). The ECR of **1** is similar except that an additional peak 3C was observed (Table 1; ESI: Figure S2). Overall, in interesting contrast to related quinoxalines whose

 ©ARKAT USA, Inc

hydrodechlorination proceeds via RAs,[32] that of studied thiadiazoles involves DAs and their protonation (Scheme 1).

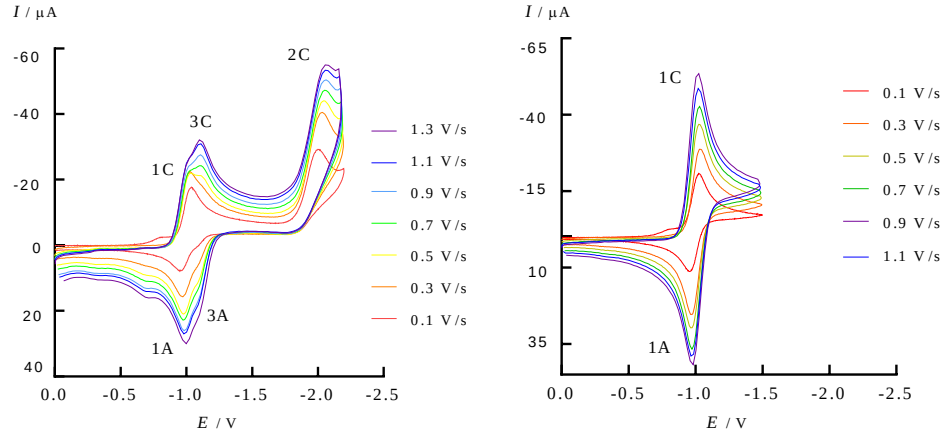

Figure 2. CV of **2** in DMF in the potential ranges 0 > E > −2.2 V (left) and 0 > E > −1.5 V (right) at different sweep rates indicated by color.

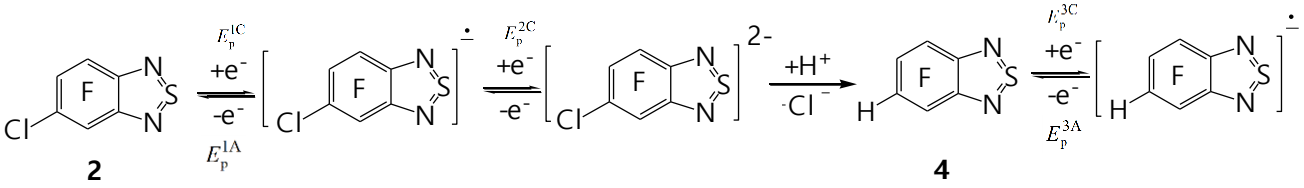

Scheme 1. Two-electron ECR hydrodechlorination of **2** followed by one-electron ECR of its product **4**.

Similarly, peak 1C of selenadiazoles **10-20** (Table 1) is one-electron, diffusion-controlled and reversible, *i.e.* corresponding to the formation of long-lived RAs (for **11** and **12**, see Figure 3; for the other, ESI: Figures S1 and S2, Table S1). Peaks 2C and 3C, however, are essentially irreversible for all **10-20**, and peak 2C is more than one-electron (I_p^{2C}/I_p^{1C} > 1, Figure 3; ESI, Figure S2).

For **12** in the range 0 > E > −2.2 V, reversible one-electron peaks 4C and 4A (E_p^{4C} = −1.45, E_p^{4A} = −1.39 V) were observed at the second cycle of potential sweep, whereas no additional peaks were detected in the range 0 > E > − 1.7 V (Figure 3). The peaks were attributed to one-electron ECR of the product resulted from defluorination of **12**. Importantly, no additional peaks in the second sweep cycle in the range $E_p^{2C} < E < E_p^{1C}$ were detected for **14**-**17** with non-halogen substituents in the positions 5 and 6, whereas weak ones were observed in anode branches of the CVs of **13**, **18** and **19** with F atoms in the position 6 (ESI: Figure S2). Altogether, these suggest that defluorination of **12** occurs regioselectively at equivalent positions 5 / 6 not involving the positions 4 / 7 (note that in fluorinated selenadiazoles the positions 5 and 6 are much more active in nucleophilic substitution than the positions 4 and 7).[29] This is, however, only minor process because peaks 4C and 4A are characterized by substantially lower currents as compared with the first peaks in CVs (Figure 3).

©ARKAT USA, Inc

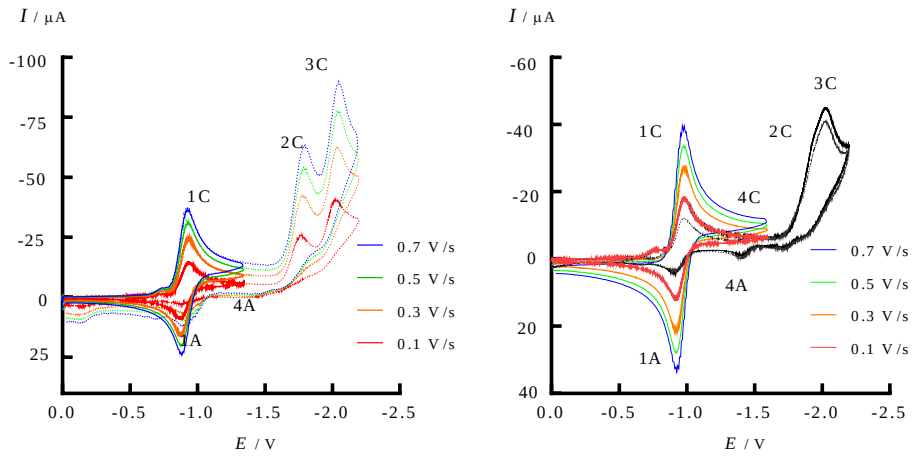

Figure 3. Left: CVs of **11** in the potential ranges 0 > *E* > −1.5 V (solid lines) and 0 > *E* > −2.2 V (dotted lines) at different sweep rates indicated by color. Right: CV of **12** in the potential ranges 0 > *E* > −1.7 V at different sweep rates, and 0 > *E* > −2.2 V at 100 mV·s^{-1} (black solid and dotted lines correspond to the first and second cycles, respectively).

Under conditions of stationary electrolysis of **12** at the E_p^{2C} potential, a RA was detected whose EPR hyperfine splitting (hfs) featured two nuclei with spin 1 and three with spin ½ thus indicating the absence of either H or F atom in the position 5/6. As compared with EPR spectra of RAs of **1**-**20** in DMF at T = 295 K (below), the spectrum of this RA revealed broadened high-field lines in nitrogen hfs suggesting modulation of ^{14}N anisotropic hyperfine interaction caused by its slower rotational diffusion. The latter can be associated with the presence of a multi-atom substituent R in the position 5/6 of the RA. The nature of R is unclear, it is not HO or Me_2N Special experiments shown that with HO^- (*e.g.* originated from protonation of DA of **12** by H_2O; *cf.* ref. 33) nucleophilic substitution in **12** does not proceed even under much drastic conditions; with Me_2NH (from decomposition of DMF under basic conditions), RA of **16** should be seen with EPR. Therefore, only structure **21** can be assigned to the discussed RA in tentative explanation of the chemistry observed (Scheme 2) requiring further investigation. In any way, one can conclude that ECR defluorination of **12** differs from that of its S congener **3** proceeded as *hydro*defluorination.[2]

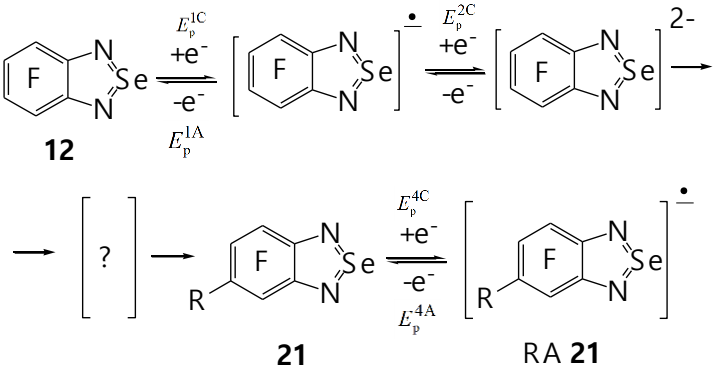

Scheme 2. Tentative explanation of defluorination of **12** with the formation of **21** followed by its one-electron reduction; R ≠ H, F, HO, Me_2N.

©ARKAT USA, Inc

First electrochemical potentials and gas-phase electron affinities. The E_p^{1C} values of selenadiazoles are *ca.* 0.1 ± 0.03 V less negative, and EA_1 *ca.* 0.17 eV more positive, than those of thiadiazoles with the same substitution patterns (Table 1, pairs **1**/**10**, **2**/**11**, **3**/**12**, **5**/**13**, **6**/**14**, **8**/**16** and **9**/**17**). They form two independent linear regressions $EA_1 = a E_p^{1C} + b$ (Figure 4) with *a, b* and r^2 equal to 1.79 eV·V^{-1}, 3.50 eV and 0.972, respectively, for thiadiazoles **1**-**9**; and to 1.61 eV·V^{-1}, 3.30 eV and 0.948 for selenadiazoles **10**-**19**; *r* is correlation coefficient. The values of *a* and *b* for both regressions are comparable with those for related compounds whose E_p^{1C} were measured in MeCN.[2]

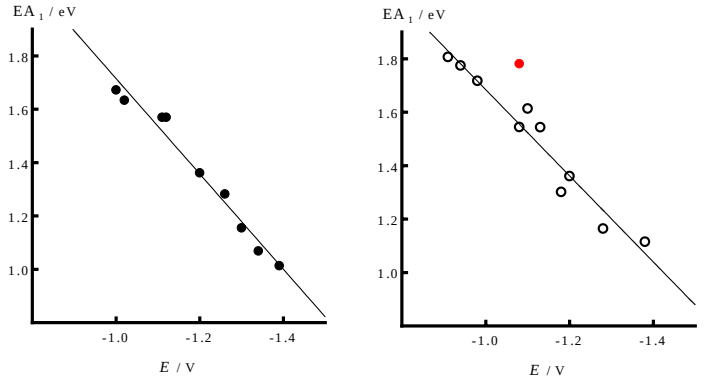

Figure 4. Correlation between EA_1 and E_p^{1C} for thiadiazoles **1**-**9** (left) and selenadiazoles **10**-**19** (right); **20** (red point) is not included due to another scaffold topology.

Altogether, these findings indicate that, in spite of lesser atomic EA_1 and Allen electronegativity of Se (2.02 and 2.42) vs. S (2.08 and 2.59), selenadiazoles are better electron acceptors than their S congeners. Earlier, this property was pointed with B3LYP calculations, and with MP2 ones it was shown that the result is not an artifact of the DFT approach.[3] Now this non-trivial trend (covering also Te congeners of compounds under discussion)[3] received experimental electrochemical confirmation. Tentatively, it might be explained by better charge/spin delocalization in the RAs of Se derivatives caused by more diffuse 4p-AO of Se as compared with 3p-AO of S.

For compounds with electron-donating substituents MeO and Me_2N, E_p^{1C} and EA_1 values reveal additivity under their accumulation. Thus, for MeO-substituted thiadiazoles **5** and **6**, the negative shifts of the E_p^{1C} relative to that of the parent **3** are −0.09 (one MeO) and −0.19 V (two MeO), respectively; for Me_2N-substituted thiadiazoles **8** and **9** the corresponding shifts are −0.15 and −0.28 V (Table 1). For selenadiazoles, the additivity of such shifts is more exact to be −0.10, −0.20, −0.40 V for MeO-substituted **13**, **14** and **15** in relation to E_p^{1C} of the parent **12**; and −0.15 and −0.30 V for Me_2N-substituted **16** and **17** (Table 1). Previously, the additivity of E_p^{1C} was observed for benzenes and naphthalenes on accumulation of electron-withdrawing substituents CF_3.[34] The present work, therefore, generalizes the trend.

EPR of radical anions. The EPR and DFT data of ECR generated (DMF, 295 K) RAs **1**-**21** are represented in Table 2 and Figs. 5 and 6; the EPR spectrum of product of ECR of **3** in MeCN was reported earlier.[2] Experimental and DFT-calculated isotropic hyperfine coupling (hfc) constants are in reasonable agreement.

Table 2. Experimental in DMF and gas-phase DFT-calculated isotropic hfc constants (G) of RAs **1**-**21**[a]

©ARKAT USA, Inc

RA	Experiment	(U)B3LYP/6-31+G(d)
1	4.30 (N^1), 5.56 (N^3), 6.92 (F^4), 3.62 (F^6), ~0.09 (Cl^5), ~0.18 (Cl^7)	4.60 (N^1), 6.06 (N^3), 8.02 (F^4), 2.61 (F^6)
2	4.80 (N^1), 5.65 (N^3), 5.41 (F^4), 2.86 (F^6), 4.19 (F^7), ~0.19 (Cl^5)	5.20 (N^1), 6.16 (N^3), 6.48 (F^4), 1.26 (F^6), 4.70 (F^7)
3[b]	5.46 ($N^{1,3}$), 4.82 ($F^{4,7}$), 4.78 ($F^{5,6}$)	5.75 ($N^{1,3}$), 5.04 ($F^{4,7}$), 2.49 ($F^{5,6}$)
4	4.81 (N^1), 5.97 (N^3), 4.25 (F^4), 1.54 (H^5), 2.67 (F^6), 3.20 (F^7)	5.10 (N^1), 6.45 (N^3), 5.85 (F^4), −1.71 (H^5), 1.69 (F^6), 4.02 (F^7)
5	5.28 (N^1), 5.52 (N^3), 4.06 (F^4), 3.86 (F^6), 4.06 (F^7)	5.49 (N^1), 6.03 (N^3), 5.25 (F^4), 2.14 (F^6), 4.47 (F^7)
6	5.47 ($N^{1,3}$), 3.37 ($F^{4,7}$), 2.05 ($^{13}C^{3a,7a}$), 2.03 ($^{13}C^{4,7}$)	5.74 ($N^{1,3}$), 4.69 ($F^{4,7}$), −5.14 ($^{13}C^{3a,7a}$), 5.07 ($^{13}C^{4,7}$)
7	5.29 (N^1), 5.65 (N^3), 3.37 (F^4), 2.99 (F^7), ~0.10 (N^{NMe2})	5.40 (N^1), 6.20 (N^3), 5.73 (F^4), 3.95 (F^7), −0.20 (N^{NMe2})
8	5.12 (N^1), 5.73 (N^3), 4.06 (F^4), 3.39 (F^6), 3.52 (F^7), 0.11 (N^{NMe2})	5.12 (N^1), 6.31 (N^3), 5.72 (F^4), 1.43 (F^6), 4.16 (F^7), −0.31 (N^{NMe2})
9	5.49 ($N^{1,3}$), 3.04 ($F^{4,7}$), 0.18 (N^{NMe2})	5.80 ($N^{1,3}$), 4.95 ($F^{4,7}$), −0.19 (N^{NMe2})
10[c,d]	4.92 (N^1), 6.26 (N^3), 5.94 (F^4), 3.73 (F^6)	4.73 (N^1), 6.21 (N^3), 6.99 (F^4), 2.89 (F^6)
11	5.44 (N^3), 6.30 (N^1), 4.56 (F^4), 2.94 (F^6), 3.27 (F^7), ~0.06 (Cl)	5.30 (N^1), 6.24 (N^3), 5.58 (F^4), 1.52 (F^6), 3.82 (F^7)
12	5.96 ($N^{1,3}$), 4.37 ($F^{4,7}$), 3.70 ($F^{5,6}$)	5.84 ($N^{1,3}$), 3.36 ($F^{4,7}$), 2.61 ($F^{5,6}$)
13	5.90 (N^1), 6.13 (N^3), 4.04 (F^4), 2.98 (F^6), 3.25 (F^7)	5.58 (N^1), 6.12 (N^3), 4.40 (F^4), 2.34 (F^6), 3.61 (F^7)
14	6.05 ($N^{1,3}$), 2.06 ($F^{4,7}$)	5.83 ($N^{1,3}$), 3.84 ($F^{4,7}$)
15	5.964 ($N^{1,3}$)	5.69 ($N^{1,3}$)
16	5.73 (N^1), 6.31 (N^3), 3.66 (F^4), 2.54 (F^6), 3.27 (F^7), 0.17 (N^{NMe2})	5.22 (N^1), 6.40 (N^3), 4.88 (F^4), 1.80 (F^6), 3.28 (F^7), −0.28 (N^{NMe2})
17	6.04 ($N^{1,3}$), 2.33 ($F^{4,7}$), 0.20 ($2N^{NMe2}$)	5.84 ($N^{1,3}$), 4.01 ($F^{4,7}$), −0.22 ($2N^{NMe2}$)
18	5.68 (N^1), 6.33 (N^3), 3.57 (F^4), 2.64 (F^6), 3.45 (F^7), 0.13 (N^{NC4H8O})	5.21 (N^1), 6.45 (N^3), 5.48 (F^4), 1.77 (F^6), 3.22 (F^7), −0.23 (N^{NC4H8O})
19	5.79 (N^1), 6.23 (N^3), 3.88 (F^4), 2.61 (F^6), 3.07 (F^7)	5.17 (N^1), 6.40 (N^3), 5.02 (F^4), 1.74 (F^6), 3.27 (F^7), −0.33 (N^{NC4H8})
20	5.77 (N^1), 5.34 (N^3), 3.24 (F^4), 0.67 (F^5), 0.33 (F^6), 2.41 (F^7), 2.84 (F^8), 2.82 (F^9)	5.34 (N^1), 5.25 (N^3), 4.39 (F^4), 1.63 (F^5), −0.69 (F^6), 1.87 (F^7), 3.23 (F^8), −2.03 (F^9)
21[e]	6.09 (N), 6.06 (N), 4.35 (F), 1.67 (F), 1.56 (F)	

[a] Numbers of RAs correspond to those of their neutral precursors; numbers of atoms H and F are the same as for C atoms they are bound with (Figure 1). [b] The EPR spectrum of RA **3** for MeCN was reported earlier.[2] [c] Hfc constants with ^{35,37}Cl nuclei are small and result only inhomogeneous line broadening. [d] EPR spectrum was simulated as a superposition of spectra of RA **10** (90%) and RA of its 5-H congener from hydrodechlorination (10%); hfs: 3N × 3N × 2F × 2F × 2H × 4Cl; hfc constants (G): $a_{N(1,3)}$ = 6.42, 4.53; $a_{F(4)}$ = 4.92; $a_{F(6)}$ = 2.06; $a_{H(5)}$ = 1.16; $a_{Cl(7)} \approx 0.2$. [e] RA **21** was obtained from ECR defluorination of **12** (Scheme 2).

©ARKAT USA, Inc

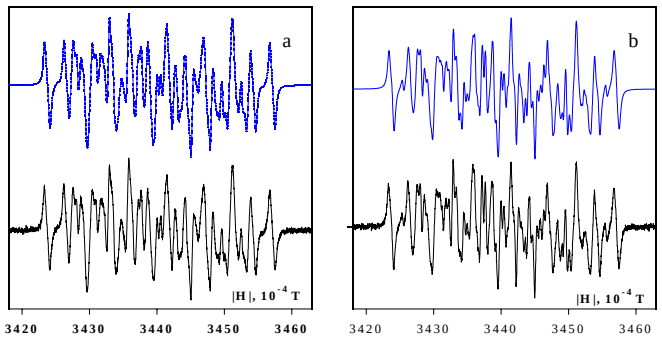

Figure 5. (a) The EPR spectrum of RA **2** in DMF and (b) its transformation when the stationary electrolysis potential is decreased to $E_{\mathrm{p}}^{2\mathrm{C}}$.

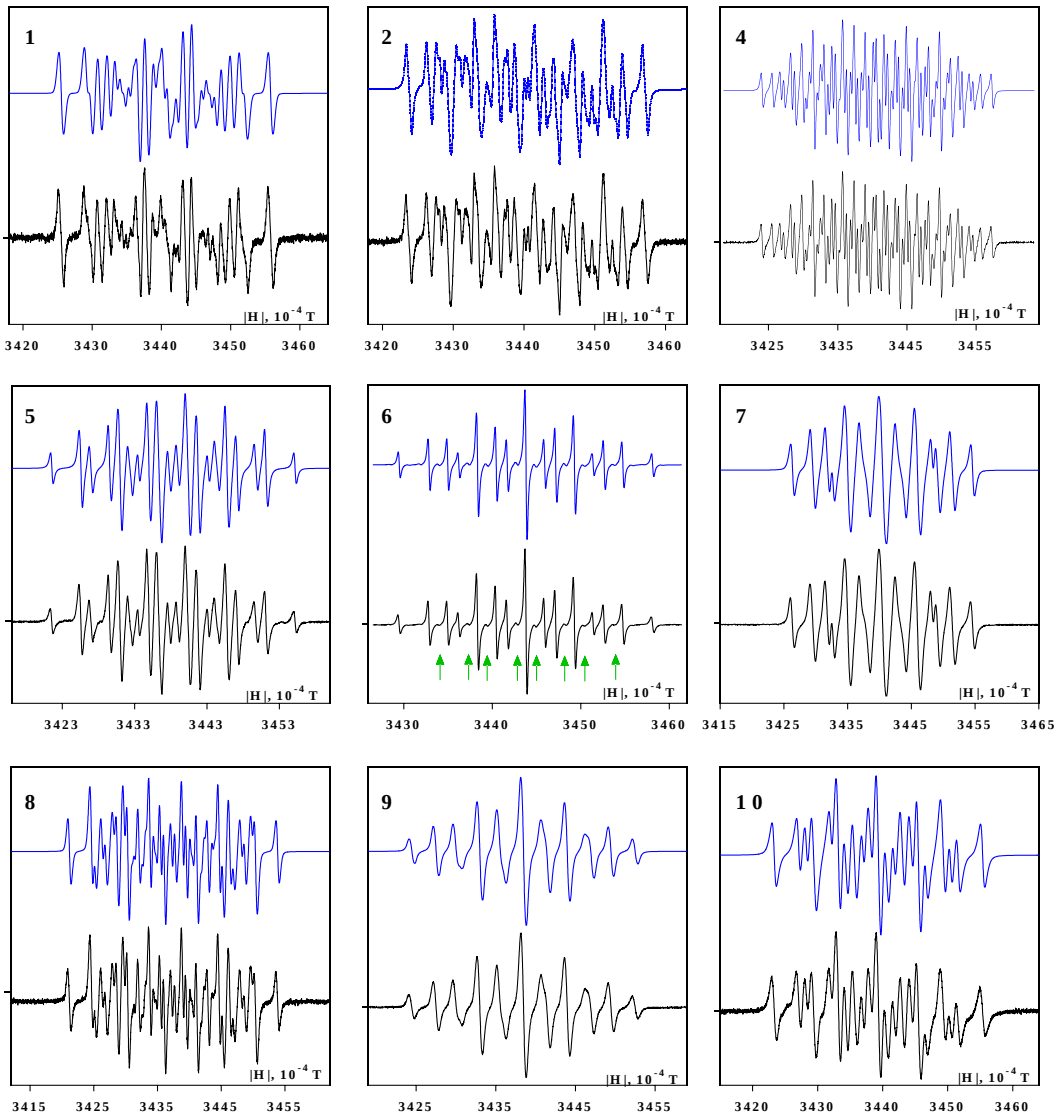

©ARKAT USA, Inc

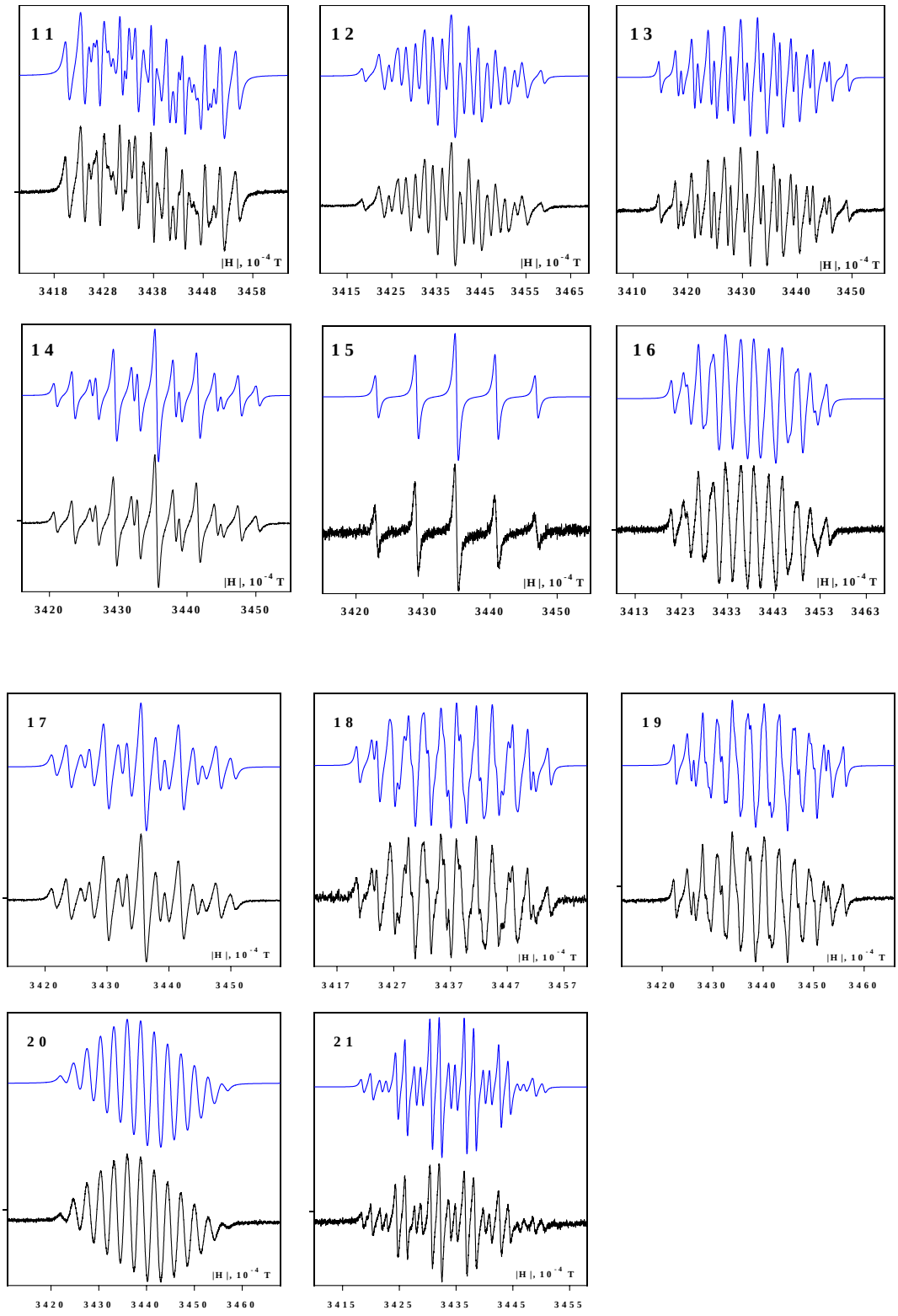

Figure 6. EPR spectra of RAs **1**, **2** and **4-21** in DMF, experiment (black) and simulation (blue). For RA **6**, green arrows indicate hfs from ^{13}C nuclei (the positions 3a, 4, 7 and 7a) at their natural abundance. EPR spectrum of RA **21** was obtained under ECR of **12** at the potential of peak 2C (Figure 3); that of RA **3** in MeCN was reported.[2]

©ARKAT USA, Inc

Except for **2** and **12**, EPR spectra were measured under conventional conditions and attributed to primary RAs of the compounds. EPR spectrum of RA **2** (Figure 5, Table 2) was obtained with stationary electrolysis in the potential range E_p^{1C} > E > −1.8 V (Figure 2); at the electrolysis potential decreased to E_p^{2C} or more, the spectrum was assigned as superposition of spectra of RAs **2** (90%) and **4** (10%). This proves the suggested two-electron mechanism of the hydrodechlorination of **2** in DMF with the participation of corresponding DA (Scheme 1). RAs of the other chlorine containing compounds **1**, **10** and **11** (Table 2), possessing more positive EA_1 than **2** (Table 1), were much stable; in any way, their possible transformations associated with the dechlorination were not detected. Stationary electrolysis of **12** at the potential E_p^{1C} (Figure 3) resulted in its RA whose identity was confirmed by EPR and DFT (Figure 6, Table 2). The decrease of the potential to E_p^{2C} afforded RA **21** (Scheme 2; Figure 6, Table 2).

In some cases, the (U)B3LYP calculations overestimated Fermi-contact spin densities at ^{19}F nuclei but practically quantitatively reproduced hfc constants with ^{14}N nuclei (Table 2). According to the calculations, all RAs are planar as expected for the π-species (Figure 7, examples for RAs **2** and **11**). Due to this, the hfc constants with ^{35,37}Cl nuclei are determined by spin-polarization mechanism of hyperfine interaction and, therefore, small in magnitude (Table 2, RAs **1**, **2**, **10** and **11**).

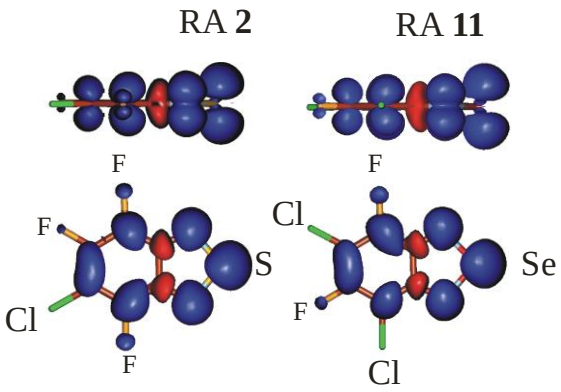

Figure 7. Spin density distributions in RAs **2** and **11** from the (U)B3LYP/6-31+G(d) calculations, color code: blue positive, red negative.

For RA **6**, the most long-lived among the studied RAs, the hfs from ^{13}C nuclei was observed at their natural abundance (Figure 6). The resolved hfc constants with ^{13}C nuclei in the positions 3a, 4, 7 and 7a are practically equal, whereas those with nuclei in the positions 5 and 6 are small and not resolved. DFT suggests negative hfc constants with ^{13}C nuclei for the positions 3a and 7a and positive ones for the positions 4 and 7 for all studied RAs (for typical examples, see Figure 7). It should be noted that the hybrid functional B3LYP *ca.* 2.5 times overestimates Fermi-contact spin densities at ^{13}C nuclei, and that the calculated hfc constants with ^{13}C nuclei are almost equal which agrees with the experimental data (Table 2).

Conclusions

In DMF, the first stage of ECR of fluorinated/chlorinated 2,1,3-benzothia/selenadiazoles **1**-**20** (bearing also substituents MeO or R_2N) is one-electron reversible process giving long-lived RAs whose authenticity is

©ARKAT USA, Inc

confirmed by EPR spectroscopy and DFT calculations at the (U)B3LYP/6-31+G(d) level of theory. The ECR first-peak potentials correlate well with gas-phase calculated EAs forming independent linear regressions for S and Se compounds. The potentials of selenadiazoles are less negative, and EAs more positive, than those of thiadiazoles; in contrast to the atomic EAs and Allen electronegativities, this suggests better electron-acceptor ability of Se derivatives which may be used in the design and synthesis of molecular functional materials.

At the second stage of ECR, *hydro*dechlorination of thia/selenadiazoles proceeds via corresponding DAs and their protonation. *Non-hydro*defluorination of selenadiazoles at the same stage, involves reductive activation by two or more transferred electrons. These dehalogenations differ from those of related aromatics (benzenes, naphthalenes)[35,36] and aza-aromatics (quinoxalines)[32] controlled by instability of their RAs, and therefore are of interest to organic chemistry.

Experimental Section

General. ^{1}H (300.13 MHz) and ^{19}F (282.36 MHz) NMR spectra were measured with Bruker AV-300 spectrometer for solutions in $CDCl_3$; standards were TMS and C_6F_6 ($\delta^{19}F$ = −162.9 with respect to $CFCl_3$). High-resolution MS spectra (EI, 70 eV) were obtained with DFS Thermo Electron instrument. UV-Vis spectra were collected with Varian Cary 5000, and fluorescence (FL) spectra with Varian Cary Eclipse, spectrophotometers, respectively, for solutions in heptane. Elemental analyses for C, H and N were performed with Carlo Erba Model 1106 instrument, and those for F by standard spectrophotometric method with Ln complex of alizarin complexone. Studied compounds **1**-**17** and **20** were synthesized by known methods (Scheme 3)[29,30,37] and compounds **18** and **19** in a similar way (below).

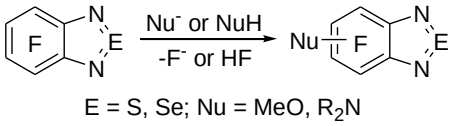

E = S, Se; Nu = MeO, R_2N

Scheme 3. Synthesis of non-chlorinated studied compounds by nucleophilic substitution of fluorine in the archetypal **3** (E = S) and **12** (E = Se). Chlorinated derivatives were prepared by cyclizing corresponding 1,2-diaminobenzenes with $SOCl_2$ or SeO_2.[29,30,37]

Cyclic voltammetry. The CV measurements on compounds **1**-**20** in DMF (1–2.6 mM solutions) were performed at 295 K in an argon atmosphere. The supporting electrolyte was 0.1 M Et_4NClO_4. A PG 310 USB potentiostat (HEKA Elektronik GmbH, Germany) was used for the measurements. A standard electrochemical cell with solution volume of 5 ml connected to the potentiostat with a three-electrode scheme was employed. A stationary Pt electrode (S = 0.064 cm^2) was used as a working electrode, and Pt helix as an auxiliary electrode. Peak potentials were quoted with reference to a saturated calomel electrode (SCE). The potential sweep rates were 0.05–1.3 $V{\cdot}s^{-1}$.

EPR spectroscopy. The EPR spectra of RAs were recorded with an ELEXSYS E-540 spectrometer (X-band, MW frequency ~9.87 GHz, MW power 1 mW, modulation frequency 100 kHz, and modulation amplitude 0.006 mT) equipped with a high-Q cylindrical resonator ER4119HS. For the EPR measurements, stationary ECR of compounds **1**-**20** at corresponding potentials of the first reduction peaks was carried out at 295 K under anaerobic conditions. Electrochemical cell for EPR measurements equipped with Pt working electrode was placed into the EPR cavity. Electrolysis was performed in a dry DMF with 0.1 M Et_4NClO_4 as a supporting

 ©ARKAT USA, Inc

electrolyte. Simulations of the experimental EPR spectra were accomplished with the *Winsim 2002* program.[38] The *Simplex* algorithm was used for optimization of hfc constants and line widths.

DFT calculations. The DFT calculations on compounds **1**-**20** and their RAs were performed with full geometry optimization at the (U)B3LYP/6-31+G(d) level of theory using the *GAMESS* program.[39] For all studied RAs the value S^2 did not exceed 0.76.

5-(Morpholin-4-yl)-4,6,7-trifluoro-2,1,3-benzoselenadiazole (18). Stirred solution of 100 mg (0.39 mmol) of **12** and 86 mg (0.39 mmol) of morpholine in 6 ml of toluene was kept at 70 °C for 12 h, cooled to ambient temperature and passed through silica column, eluent toluene. The eluate was evaporated under reduced pressure, and the residue recrystallized from 2:1 hexane / toluene. Compound **18** was obtained in the form of yellow crystals, yield 82 mg (65%), mp 234-235 °C. Elemental analysis for $C_{10}H_8F_3N_3OSe$ (%): found: 37.74 (C); 2.18 (H); 12.89 (N); 17.24 (F); calculated: 37.28 (C); 2.50 (H); 13.04 (N); 17.69 (F). MS, *m/z*: 322.9776 $[C_{10}H_8F_3N_3O^{80}Se]^+$ (calculated 322.9779). NMR (ESI, Figure S3), δ: ^{1}H: 3.22 (m, 4H), 3.84 (m, 4H); ^{19}F: 22.1 (d, F-4, *J* 19 Hz), 19.8 (d, F-6, *J* 13.8 Hz), 11.1 (dd, F-7, *J* 19, *J* 13.8 Hz). UV-Vis, λ_{max}, nm, (log ε): 326 (4.12). FL, λ_{max} (λ_{ex}), nm: 454 (372).

5-(Pyrrolidin-1-yl)-4,6,7-trifluoro-2,1,3-benzoselenadiazole (19). Stirred solution of 100 mg (0.39 mmol) of **12** and 28 mg (0.39 mmol) of pyrrolidine in 5 ml of toluene was kept at 65 °C for 15 h, cooled to ambient temperature and passed through silica column, eluent toluene. The eluate was evaporated under reduced pressure, and the residue recrystallized from 5 ml of toluene. Compound **19** was obtained in the form of yellow crystals, yield 89 mg (74%), mp 178-179 °C. Elemental analysis for $C_{10}H_8F_3N_3Se$ (%): found: 38.99 (C); 2.59 (H); 13.48 (N); 18.87 (F); calculated: 39.23 (C); 2.63 (H); 13.73 (N); 18.62 (F). MS, *m/z*: 306.9831 $[C_{10}H_8F_3N_3{}^{80}Se]^+$ (calculated 306.9830). NMR (ESI, Figure S4), δ: ^{1}H: 1.96 (m, 4H), 3.71 (m, 4H); ^{19}F: 21.6 (m, F-4), 14.2 (m, F-6), 10.2 (dd, F-7; *J* 16.8, *J* 12.1 Hz). UV-Vis, λ_{max} (log ε): 258 (4.11), 340 (3.86), 444 (3.70). FL, λ_{max} (λ_{ex}), nm: 510 (445).

Interaction of 12 with KOH in DMF. At ambient temperature, a stirred solution of 100 mg (0.39 mmol) of **12** and 22.4 mg (0.39 mmol) of KOH in 5 ml of DMF was kept for 72 h. Despite dark color of the reaction mixture, NMR revealed only starting **12** (δ^{19}F: 13.0, 5.6). After 8 h at 80 °C, compound **16**[28] (*i.e.* product of substitution of F with Me_2NH from decomposition of DMF) was detected (δ^{19}F: 21.7, 19,7, 10.2) together compound **12**; product of the substitution with HO^- was not observed.

Acknowledgements

The authors are grateful to the Multi-Access Center *Chemical Service*, Siberian Branch of the Russian Academy of Sciences, for instrumental facilities.

Supplementary Material

See **Figure S1.** Linear dependences I_p^{1C} vs. $\nu^{1/2}$ proving diffusion-controlled nature of the first peaks of ECR of **1**, **2** and **4**-**20**. **Table S1.** Parameters of linear regressions $I_p^{1C} = A \cdot \nu^{1/2} + B$ for **1**, **2** and **4**-**20**[a]. **Figure S2.** CVs of **1**, **4-10** and **13-20** at different potential sweep rates. **Figure S3**. NMR spectra of the compound **18**. **Figure S4**. NMR spectra of the compound **19.**

References

©ARKAT USA, Inc

1. Boere, R. T.; Roemmele, T. L. *Coord. Chem. Rev.* **2000**, *210*, 369-445. https://doi.org/10.1016/S0010-8545(00)00349-0
2. Vasilieva, N. V.; Irtegova, I. G.; Gritsan, N. P.; Lonchakov, A. V.; Makarov, A. Yu.; Shundrin, L. A.; Zibarev, A. V. *J. Phys. Org. Chem.* **2010**, *23*, 536-543. https://doi.org/10.1002/poc.1637
3. Lonchalov, A. V.; Rakitin, O. A.; Gritsan, N. P.; Zibarev, A. V. *Molecules* **2013**, *18*, 9850-9900. https://doi.org/10.3390/molecules18089850
4. Neto, B. A. D.; Lapis, A. A. M.; de Silva Junior, E. N.; Dupont, J. *Eur. J. Org. Chem.* **2013**, *2013*, 228-255. https://doi.org/10.1002/ejoc.201201161
5. Todress, Z. V. *Chalcogenadiazoles: Chemistry and Applications*. CCR Press / Taylor & Francis: London, 2012.
6. Koutentis, P. A. *Comprehensive Heterocyclic Chemistry III*. Eds. Katritzky, A. R.; Ramsden, C. A.; Scriven, E. F. V.; Taylor, R. J. K.; Elsevier: Oxford, 2008; Vol. 5, pp 516-564.
7. Koutentis, P. A. *Science of Synthesis.* Eds. Storr, R. C.; Gilchrist, T. L.; Thieme: Stuttgart, 2003; Vol. 13, pp 297-348.
8. Semenov, N. A.; Bagryanskaya, I. V.; Alekseev, A. V.; Gatilov, Yu. V.; Lork, E.; Mews, R.; Roeschentaler G.V.; Zibarev A. V. *J. Struct. Chem.* **2010**, *51*, 552-557. https://doi.org/10.1007/s10947-010-0080-5
9. Bashirov, D. A.; Sukhikh, T. S.; Kuratieva, N. V.; Chulanova, E. A.; Yushina, I. V.; Gritsan, N. P.; Konchenko, S. N.; Zibarev A. V. *RSC Advances* **2014**, *4*, 28309-28316. https://doi.org/10.1039/c4ra03342f
10. Bashirov, D. A.; Sukhikh, T. S.; Kuratieva, N V.; Naumov, D. Yu.; Konchenko, S. N.; Semenov, N. A.; Zibarev, A. V. *Polyhedron* **2012**, *42*, 168-174. https://doi.org/10.1016/j.poly.2012.05.015
11. Konchenko, S. N.; Gritsan, N. P.; Lonchakov, A. V.; Radius, U.; Zibarev, A.V. *Mendeleev Commun.* **2009**, *19*, 7-9. https://doi.org/10.1016/j.mencom.2009.01.003
12. Semenov, N. A.; Pushkarevsky, N. A.; Suturina, E. A.; Chulanova, E. A.; Kuratieva, N. V.; Bogomyakov, A. S.; Irtegova, I.G.; Vasilieva, N. V.; Konstantinova, L. S.; Gritsan N. P.; Rakitin, O. A.; Ovcharenko, V. I.; Konchenko, S. N.; Zibarev, A. V. *Inorg. Chem.* **2013**, *52*, 6654-6663. https://doi.org/10.1021/ic400659q
13. Zhang, X.; Bronstein, H.; Kronemeijer, A. J.; Smith, J.; Kim, Y.; Kline, R. J.; Richter, L. J.; Antopoulos, T. D.; Sirringhaus, H.; Song, K.; Heeney, M.; Zhang, W.; McCulloch, I.; DeLongchamp, D. M. *Nature Commun.* **2013**, *4*, 2238.
14. Tsao, H. N.; Cho, D. M.; Park, I.; Hansen, M. R.; Mavrinsky, A.; Yoon, D. Y.; Graf, R.; Pisula, W.; Spiess, H. W.; Muellen, K. *J. Am. Chem. Soc.* **2011**, *133*, 2605-2612. https://doi.org/10.1021/ja108861q
15. Nielsen, C. B.; Schoeder, B. C.; Hadipour, A.; Rand, B. P.; Watkins, S. E.; McCulloch, I. *J. Mater. Chem.* **2011**, *21*, 17642-17645. https://doi.org/10.1039/c1jm13393d
16. Mancilha, P. S.; Barloy, L.; Rodembusch, F. S.; Dupont, J.; Pfeffer, M. *Dalton Trans.* **2011**, *40*, 10535-10544. https://doi.org/10.1039/c1dt10666j
17. Thomas, K. R. J.; Lin, J. T.; Velusamy, M.; Tsao, Y. T.; Chuen, C. H. *Adv. Funct. Mater.* **2004**, 14, 83-90. https://doi.org/10.1002/adfm.200304486

 ©ARKAT USA, Inc

18. Zang, X.; Gorohmaru, H.; Kadowaki, M.; Kobayashi, T.; Ishii, T.; Tiemann, T.; Mataka, S. *J. Mater. Chem.* **2004**, *14*, 1901-1904. https://doi.org/10.1039/B402645D
19. Hou, Q.; Zhou, Q.; Zhang, Y.; Yang, W.; Yang, R.; Cao, Y. *Macromolecules* **2004**, *37*, 6299-6305. https://doi.org/10.1021/ma049204g
20. Liu, J.; Zhou, Q. G.; Cheng, Y. X.; Geng, Y. H.; Wang, L. X.; Ma, D. G.; Jing, X. B.; Wang, R. S. *Adv. Funct. Mater.* **2006**, *16*, 957-965. https://doi.org/10.1002/adfm.200500761
21. Uchiyama, S.; Kimura, K.; Gota, C.; Okabe, K.; Kawamoto, K.; Inada, N.; Yoshihara, T.; Tobita, S. *Chem. Eur. J.* **2012**, 18, 9552-9563. https://doi.org/10.1002/chem.201200597
22. Neto, B. A. D.; Carvalho, P. H. P. R.; Correa, J. R. *Acc. Chem. Res.* **2015**, *48*, 1560-1569. https://doi.org/10.1021/ar500468p
23. Sukhikh, T. S.; Bashirov, D. A.; Ogienko, D. S.; Kuratieva, N. V.; Sherin, P. S.; Rakhmanova, M. I.; Chulanova, E. A.; Gritsan, N. P.; Konchenko S. N.; Zibarev, A. V. *RSC Advances*, **2016**, *6*, 43901-43910. https://doi.org/10.1039/C6RA06547C
24. Sukhikh, T. S.; Bashirov, D. A.; Kuratieva, N. V.; Smolentsev, A. I.; Bogomyakov, A. S.; Burilov, V. A.; Mustafina, A. R.; Zibarev, A. V.; Konchenko, S. N. *Dalton Trans.* **2015**, *44*, 5727-5734. https://doi.org/10.1039/C4DT03878A
25. Sukhikh, T. S.; Bashirov, D. A.; Kolybalov, D. S.; Andreeva, A. Yu.; Smolentsev, A. I.; Kuratieva, N. V.; Burilov, V. A.; Mustafina, A. R.; Kozlova, S. G.; Konchenko, S. N. *Polyhedron* **2017**, *124*, 139-144. https://doi.org/10.1016/j.poly.2016.12.041
26. Babudri, F.; Farinola, G. M.; Naso, F.; Ragni, R. *Chem. Commun.* **2007**, 1003-1022. https://doi.org/10.1039/B611336B
27. Nielsen, C. B.; White, A. J. P.; McCulloch, J. *J. Org. Chem.* **2015**, *80*, 5045-5048. https://doi.org/10.1021/acs.joc.5b00430
28. Wu, J. I.; Puehlhofer, F. G.; von Ragué Schleyer, P.; Puchta, R.; Kiran, B.; Mauksch M.; van Eikema Hommes, N. J. R.; Alkorta, I.; Elguero, J. *J. Phys. Chem. A* **2009**, *113*, 6789-6794. https://doi.org/10.1021/jp902983r
29. Mikhailovskaya, T. F.; Makarov A. G.; Selikhova N. Yu.; Makarov, A. Yu.; Pritchina, E. A.; Bagryanskaya, I. Yu.; Vorontsova, E. V.; Ivanov, I. D.; Tikhova, V. D.; Gritsan N. P.; Slizhov Yu. G.; Zibarev, A. V. *J. Fluorine Chem*. **2016**, *183*, 44-58. https://doi.org/10.1016/j.jfluchem.2016.01.009
30. Makarov, A. G.; Selikhova, N. Yu.; Makarov, A. Yu.; Malkov, V. S.; Bagryanskaya, I. Yu.; Gatilov, Yu. V.; Knyazev, A. S.; Slizhov, Yu. G.; Zibarev, A. V. *J. Fluorine Chem.* **2014**, *165*, 123-131. https://doi.org/10.1016/j.jfluchem.2014.06.019
31. *Organic Redox Systems: Synthesis, Properties, and Applications*. Ed. Nishinaga, T.; Wiley, 2016.
32. Shundrin, L. A.; Vasilieva, N. V.; Irtegova, I. G.; Avrorov, P. A.; Selikhova, N. Yu.; Makarov, A. G.; Makarov, A. Yu.; Slizhov, Yu. G.; Zibarev, A. V. *J. Phys. Org. Chem.* **2017**. https://doi.org/10.1002/poc.3667
33. Konstantinova, L. S.; Knyazeva, E. A.; Obruchnikova, N. V.; Vasilieva, N. V.; Irtegova, I. G.; Nelyubina, Yu. V.; Bagryanskaya, I. Yu.; Shundrin, L. A.; Zibarev, A. V.; Rakitin, O. A. *Tetrahedron* **2014**, *70*, 5558-5568. https://doi.org/10.1016/j.tet.2014.06.096

 ©ARKAT USA, Inc

34. Dunyashev, V. S.; Polenov, E. A.; Minina, N. E.; Kazakova, V. M.; Grigorev, G. A.; Yagupolskii, L. M. *Zh. Obshch. Khim*. (*Russ. J. Gen. Chem.*) **1988**, *58*, 200-201 (in Russian).
35. Rossi, R. A.; Pierini, A. B.; Penenory, A. B. *Chem. Rev*. **2003**, *103*, 71-167. https://doi.org/10.1021/cr960134o
36. Saveant, J. M. *Acc. Chem. Res*. **1980**, *13*, 323-329. https://doi.org/10.1021/ar50153a005
37. Zibarev, A. V.; Miller, A. O. *J. Fluorine Chem.* **1990**, *50*, 359-363. https://doi.org/10.1016/S0022-1139(00)85001-0
38. R. D. Duling, *J. Magn. Reson*. **1994**, *104*, 105-115. https://doi.org/10.1006/jmrb.1994.1062
39. Schmidt, M. W.; Baldridge, K. K.; Boatz, J. A.; Elbert, S. T.; Gordon, M. S.; Jensen, J. H.; Koseki, S.; Matsunaga, N.; Nguyen, K. A.; Su, S. J.; Windus, T. L.; Dupuis, M.; Montgomery, J. A. *J. Comput. Chem.* **1993**, *14*, 1347-1363. https://doi.org/10.1002/jcc.540141112

 ©ARKAT USA, Inc